JOURNAL OF CATALYSIS 129, 1–11 (1991)

Catalytic Hydrogenation of 1,3-Butadiene on Pd Particles Evaporated on Carbonaceous Supports: Particle Size Effect

B. TARDY,* C. NOUPA,* C. LECLERCQ,* J. C. BERTOLINI,* A. HOAREAU,† M. TREILLEUX,† J. P. FAURE,‡ AND G. NIHOUL‡

*Institut de Recherches sur la Catalyse, 2 avenue Albert Einstein, 69626, Villeurbanne Cédex; †Département de Physique des Matériaux, Université Lyon I, 69622, Villeurbanne Cédex; and ‡Groupe de Microscopie Electronique de Toulon, Université de Toulon, BP 132, 83957, La Garde Cédex, France

Received January 17, 1990; revised October 15, 1990

The catalytic activity of Pd aggregates obtained by atomic-beam vacuum deposition on carbonaceous substrates (amorphous carbon and graphite) has been measured in the 1,3-butadiene hydrogenation reaction. The particle sizes have been determined by TEM. Whatever the support, this reaction appears to be very size sensitive. Metal particles larger than 2.8 nm behave similarly to bulk palladium. The size effect is marked in the 2.8 to 1.4 nm specific diameter range. No activity remains for sizes below 1.4 nm. Highly marked deactivation processes are responsible for the main variations in the catalytic behavior. © 1991 Academic Press, Inc.

INTRODUCTION

In the course of the preparation of catalysts containing noble metals, which are very expensive materials, one expects to get highly dispersed metallic particles, i.e., in which the majority of the metal atoms constitute the surface on which the catalytic processes take place; a dispersion better than 0.5 imposes particle sizes of less than 2 nm for spherical particles. Moreover, depending upon the method of preparation, the metal crystallites will differ both in size and shape. Therefore, both the influence of the surface structure and of the size must be considered. Combined studies of the catalytic behavior of metal single crystals showing different crystallographic surface orientations and of metal particles evaporated onto a flat support (which allows production of very small particles having a sharp size distribution and can serve as a model for highly dispersed supported metal catalysts) should help for the comprehension of the structural and size effects in catalysis.

The orientation and surface structure of the deposits may depend upon the cleanliness and the orientation of the support which often induces epitaxial relationships (*1–3*). Moreover, additional strain effects can occur; for example, the Pd lattice of small Pd particles deposited on MgO is expanded relatively to the bulk (*3, 4*). The influence of the surface structure cannot be considered only as a geometrical effect; indeed, changes occur in the coordination number of the outer metal atoms, and consequently in the electronic structure associated with the surface atoms (*5*).

Modifications of the electronic properties do occur for very small particles. For metal aggregates obtained by atomic-beam deposition on supports, upward core-level binding energy shifts and widening of the photoemission lines are measured when the metal particle size is decreased; such changes become significant below 3–2.5 nm for the mean diameter of the crystallites, and are of the same order of magnitude whatever the considered metal (Pd, Pt, Au) and support (C, SiO_2, Al_2O_3) (*6*). Such variations could be the consequence of changes of the average coordination number, which would become significant for particles containing less than a hundred atoms, i.e., 1.5 nm (*6*). Changes of the chemical properties are thus

0021-9517/91 $3.00

expected for very small sizes of the metal crystallites. Indeed, in gaseous phase abrupt changes with cluster size in the chemical reactivity of Fe_n, including hydrogen chemisorption rate and binding energies with ammonia and water, have been observed in the Fe_{13}–Fe_{23} cluster size range (*7*). Moreover, it has been shown that Rh reacts with D_2 and N_2 as soon as the number of atoms in the cluster is larger than five (*8*). On supported Pd particles, the continuous increase of the adsorption energy of CO with the decreasing of the particle size below 2.5 nm is significant of the size dependence of the electronic and chemical properties of Pd (*9*). Masson *et al.* (*10*) have found that accessible platinum atoms on very small Pt particles (0.6–1.1 nm) deposited on amorphous silica hydrogenate ethylene three times as quickly as if the particles were larger than 1.1 nm; smaller particles do not. The same behavior has been evidenced whatever the support, silica or alumina (*11*), and also for Ni (*12*) and Pd (*13*).

The present work is relative to the study of the chemical behavior versus size of Pd particles vapor deposited on amorphous carbon and graphite supports. Metal particles evaporated on a flat support can serve as a model for highly dispersed metal catalysts. Advantages are easy control of particle size, easy change of support nature, good reproductibility of sample preparation by adjusting the deposition conditions, and very little contamination since the evaporation is carried out under high vacuum. Besides, particles deposited on carbonaceous supports are directly observable by transmission electron microscopy and transmission electron diffraction without having to remove the particles from the substrate for observation.

Palladium is still considered the best catalyst for the partial hydrogenation of alkynes and alkadienes. But controversies exist on the Pd size effect for such catalytic hydrogenations. On Pd/Al_2O_3 and Pd/SiO_2 catalysts, Boitiaux *et al.* (*14, 15*) found large decrease of activity for both the 1-alkyne and 1,3-butadiene hydrogenation reactions when the particle size is decreased. But, from the works of Sarkany *et al.* (*16*) and Ouchaïb (*17*) no such correlation between the particle size and the activity/selectivity of Pd can be established for such reactions. Moreover, surface structure effects are clearly evidenced from works on single crystals: the turnover frequency is largely higher on the Pd (110) surface than on the Pd (111) for the 1,3-butadiene hydrogenation (*18*).

The aim of that investigation was the study of the behavior of Pd particles of varied size obtained by vapor deposition on carbonaceous supports (amorphous carbon and pyrolytic graphite) for the 1,3-butadiene hydrogenation reaction. Vibrational EELS spectroscopy has been tentatively applied to characterize the chemical state of adsorbed carbon monoxide and unsaturated hydrocarbons. The results are compared with those obtained on Pd single crystals.

EXPERIMENTAL

Experiments were performed in an ultrahigh vacuum (UHV) system composed of three main parts. A schematic representation is given in Fig. 1.

Palladium was vapor deposited on two carbonaceous supports from an atomic beam Pd source mounted in the preparation chamber. The Pd source was a Knudsen cell having characteristics close to those described by Bellamy and Colomer (*19*). The pressure during Pd evaporations was 2.7×10^{-7} Pa. A quartz microbalance was placed in front of the metal evaporator to control the metal vapor flux. The instrument was calibrated against Rutherford backscattering spectrometry (RBS) measurements. During evaporation, a collimator was put in front of the supports so that the condensation occurred only on 0.64 cm^2.

Deposits were made on two carbonaceous supports: a thin film (<10 nm thick) of amorphous carbon obtained by evaporation of C on a 1000-mesh Cu grid and a pyrolytic crys-

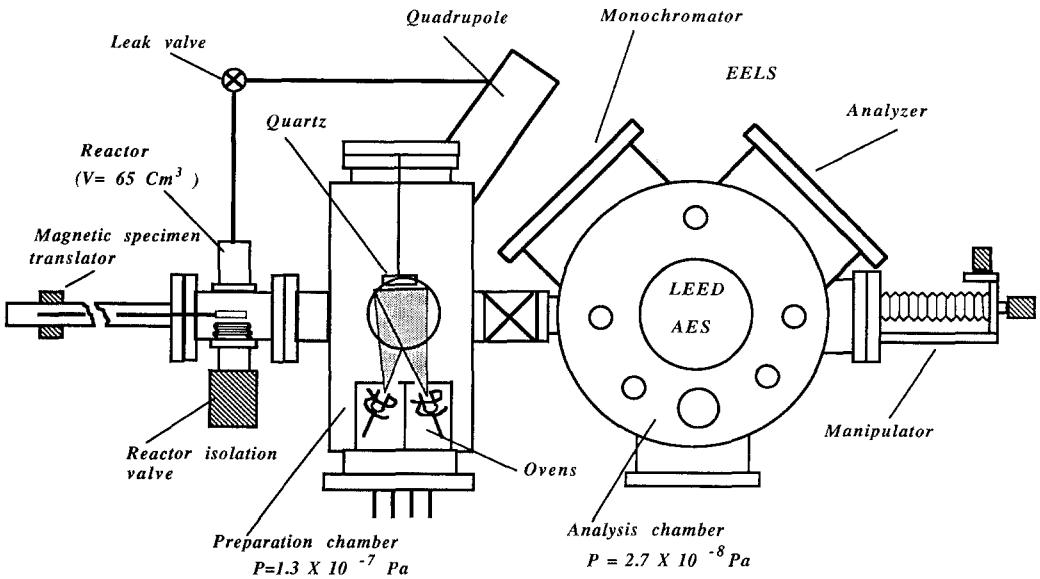

FIG. 1. Schematic representation of the UHV system used for Pd particle preparation, catalysis, and chemisorptive studies.

tal PGCCL purchased from Le Carbone-Lorraine. These substrates were outgassed many hours at 700 K under UHV conditions. Evaporations were made during 30 to 330 s on the carbonaceous substrates maintained at room temperature. The Pd deposition rate on the supports was 1.35×10^{13} atoms $\cdot$ cm^{-2} $\cdot$ s^{-1}, as determined from RBS measurements. Palladium particles of various size distributions were so obtained.

The sample was transferred under UHV conditions to a 65-cm^3 high pressure reactor. Butadiene hydrogenation was performed at room temperature under static conditions. The reaction mixture was prepared separately in a large volume cell and introduced through a large conductance valve. The composition of the reaction mixture was analyzed by mass spectroscopy, by periodic sampling through a leak valve. The relative amounts of 1,3-butadiene, butenes, and butane are determined using sensitivity factors obtained from mass spectra of pure elements. The mass spectrometer does not distinguish the different butene isomers.

The turnover frequency (TOF) is defined as the number of 1,3-butadiene molecules transformed per unit time (s^{-1}) on one metal surface atom. The number of surface atoms was calculated from the mean diameter $d_{sp} = \Sigma\, n_i d_i^3 / \Sigma\, n_i d_i^2$ of the Pd particles determined from TEM data, and assuming a spherical shape for the metal crystallites. The hypothesis of a spherical shape is consistent, since the total number of Pd atoms calculated from TEM data (i.e., N(Pd) Σ_i $1.105 n_i(\pi d_i^3/6)$) (*20*) on a given area, where N(Pd) is the number of Pd atoms per volume unit, is close to that determined from the quartz microbalance calibrated by RBS.

Before or after reaction, the samples were transferred on a $XYZ\Theta$ manipulator in the main analyzing chamber, in which RFA LEED/Auger and high resolution EELS facilities are available.

Pd particles were exposed to nitrogen and to air before observation by transmission electron microscopy (TEM JEOL 100 CX of JEOL 2000 EX and HRTEM JEOL 200 CX) or by X-ray photoemission spectroscopy (HP 5950 A ESCA spectrometer with monochromatized Al$K\alpha$ primary photon

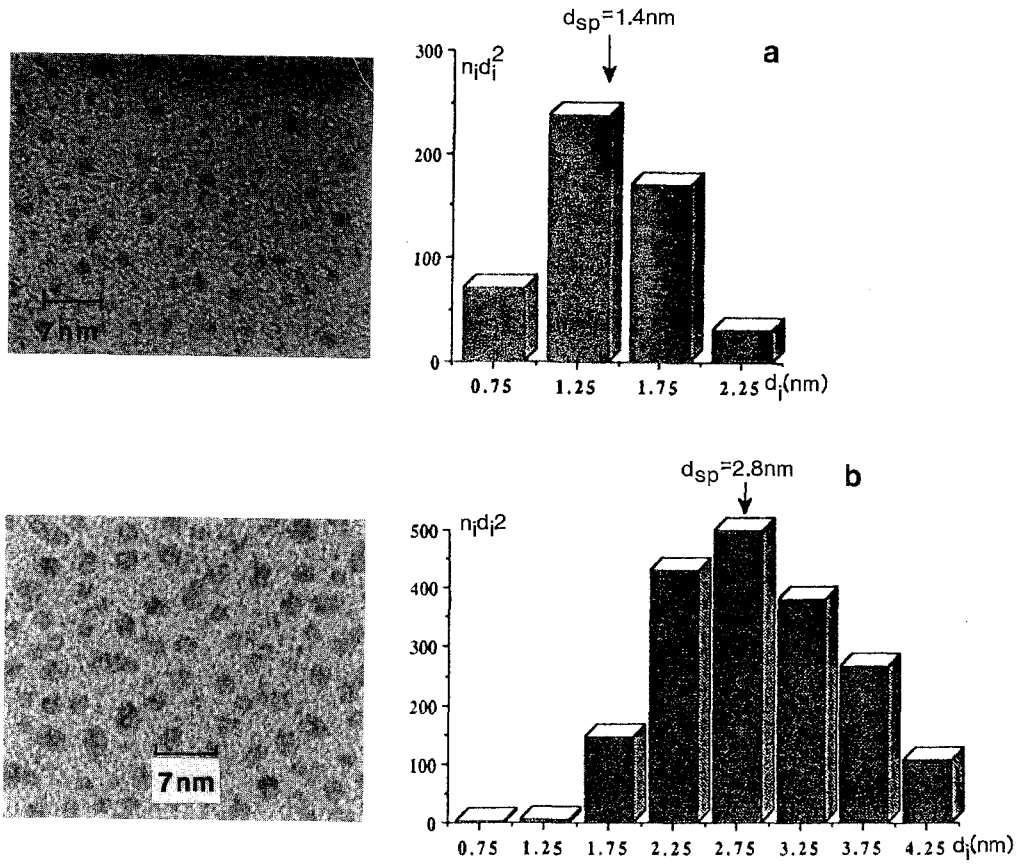

FIG. 2. (a) TEM micrograph of a Pd/amorphous carbon sample with a coverage of 4×10^{14} atoms $\cdot$ cm^{-2} and particle size distribution established from this micrograph (a mean $d_{sp} = \Sigma\, n_i d_i^3 / \Sigma\, n_i d_i^2$ of 1.4 nm corresponds to a mean $\bar{d} = \Sigma\, n_i d_i / \Sigma\, n_i$ of 1.2 nm). (b) TEM micrograph of a Pd/amorphous carbon sample with a coverage of 5×10^{15} atoms $\cdot$ cm^{-2} and particle size distribution for the same deposit (a mean d_{sp} of 2.8 nm corresponds to a mean $\bar{d}$ of 2.5 nm).

beam). All observations were made after the 1,3-butadiene hydrogenation reaction.

RESULTS

Part I. Pd Vapor Deposited on Amorphous Carbon

Electron microscopy. TEM micrographs of two deposits corresponding to the smaller and larger Pd particles are shown in Fig. 2. The size distributions were determined from these micrographs. The dependence of d_{sp} with the Pd coverage Θ is given in Fig. 3. The specific diameter d_{sp} increases roughly as the half power of the Pd coverage Θ, or of the deposition time, since the Pd flux is

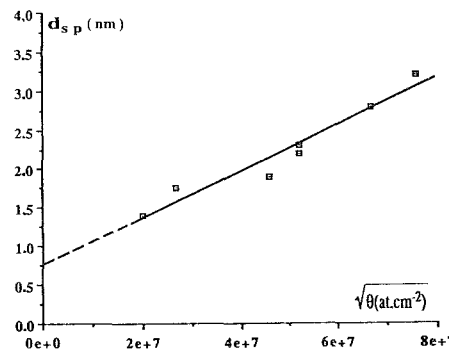

FIG. 3. Variation of the mean diameter d_{sp} of Pd particles supported by amorphous carbon versus metal coverage Θ.

constant. The particle number density of the Pd deposits is almost constant and equal to 6×10^{12} cm^{-2}.

Weak rings appear on the transmission electron diffraction patterns obtained from the Pd deposits on amorphous carbon. They correspond to all the lowest spatial frequencies of palladium: (111), (002), (202), (311), and (222). Thus all orientations of palladium particles are present with respect to the carbon substrate. Dark field images obtained from the deposit definitively prove this conclusion. Indeed with objective apertures set in different positions including either (111) ring or (002) ring or (202) ring, dark field images exhibit only some palladium particles.

Some deposits were examined by high resolution electron microscopy (HRTEM). However, taking into account the interplanar distances of palladium (in decreasing order: 0.225 nm for {111} planes, 0.195 nm for {200} planes, 0.138 nm for {220} planes, etc.) and the resolution of the JEOL 200 CX electron microscope (point image: 0.22 nm and lattice image: 0.14 nm) only the {111} and {200} lattice planes can be observed. This considerably restricts the directions of observation with "atomic resolution" of Pd particles, and explains why the majority of particles observed with atomic resolution are viewed along a ⟨110⟩ direction. In this direction, {110} planes are parallel to the substrate, while {111} planes are normal to substrate (Fig. 4a). Due to the small interplanar distance of {200} planes, only a few particles are imaged in this ⟨100⟩ direction (Fig. 4b). Some particles of larger size (>3 nm) exhibit a C_5 symmetry axis (decahedral multiply twinned particle in Fig. 4c). Optical diffractograms (Fig. 4d, 4e, 4f) performed respectively on the negative images of the

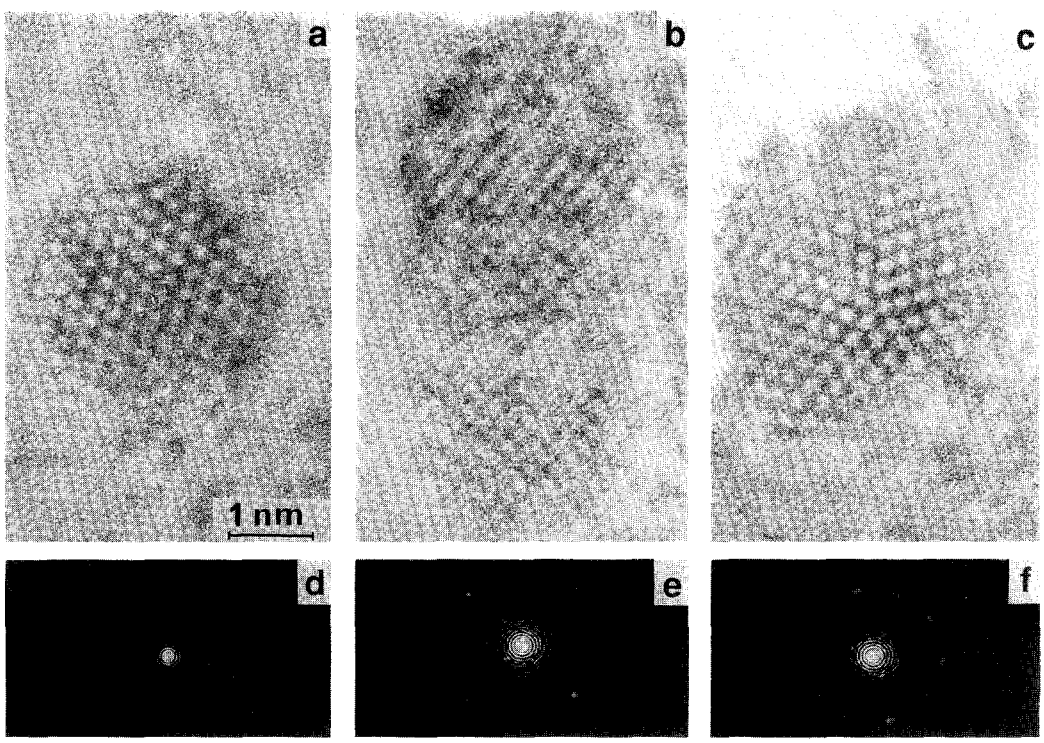

FIG. 4. High resolution images of palladium particles (2.75×10^{15} atoms · cm^{-2} Pd deposit on amorphous carbon): (a) [110] oriented, (b) [100] oriented, (c) decahedral multiply twinned; and their respective optical diffractograms d, e, f.

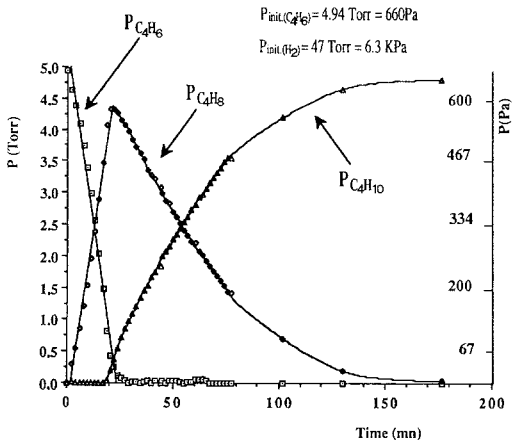

FIG. 5. Partial pressure variations of 1,3-butadiene, butenes, and butane versus time on a 4.5 × 10^{15} atoms · cm^{-2} Pd deposit on an amorphous carbon support. (P diene = 4.94 Torr = 660 Pa; P hydrogen = 47 Torr = 6.3 KPa).

particles presented in Fig. 4a, 4b, 4c are in agreement with the symmetry of palladium in the considered directions of observation.

Catalytic reaction. The variation of the partial pressures of 1,3-butadiene, butenes, and butane are given in Fig. 5 for a reaction catalyzed by a 4.5 × 10^{15} atoms · cm^{-2} Pd deposit. During the first 18 min only butenes are produced. Whatever the Pd concentration, the selectivity toward butenes remains near unity up to a very high conversion level. The initial activity per surface metal atom, measured from the diminution of the 1,3-butadiene partial pressure, increases with Pd particle size. Figure 6, shows the TOF values for Pd particles having d_{sp} diameter ranging between 1.4 and 2.8 nm. These values correspond to an extrapolation of the experimental data at 100 Torr hydrogen pressure. The order for the reaction with respect to the hydrogen pressure has been taken equal to unity (*21*). The reaction rate constancy versus the conversion level (Fig. 5) is characteristic of a zero order for the reaction with respect to the 1,3-butadiene pressure.

The reactivity of 1.4-nm Pd particles is negligible. The reaction rate increases rapidly with particle size up to a value comparable to that measured on Pd (110) single crystal surfaces (*18*). Coalescence between Pd clusters appears for d_{sp} larger than 2.8 nm. Turnover frequencies cannot be accurately measured beyond this point.

Part II. Pd Vapor Deposited on Graphite

Electron microscopy. In Fig. 7a, a TEM micrograph is shown for a Pd deposit of 8.5 × 10^{14} atoms · cm^{-2} along with the corresponding size distribution. Here again, some studies have been performed to see the orientations of the palladium particles. Electron diffraction patterns show only the graphite characteristic spots: whatever the time of exposure, we never obtained rings like the ones which were obtained from palladium deposited on amorphous carbon. In Fig. 7b the relative position of graphite (spots) and bulk palladium (rings) spatial frequencies is schematically represented. On dark field images obtained with an objective aperture placed in any of the positions I, II, III, IV, or V shown on Fig. 7b no particle can be seen. On a dark field image done with an objective aperture centered around a {11.0} graphite spot (position VI on Fig. 7b) all the palladium particles are seen. Although the dark field image is not very good

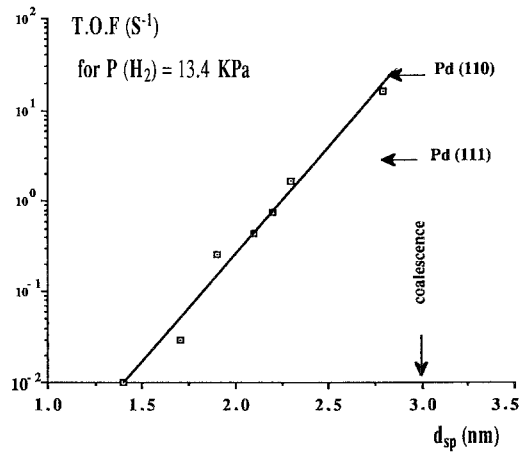

FIG. 6. Variation of the TOF with the mean diameter d_{sp} of Pd particles deposited on amorphous carbon, at 293 K and 100 Torr for the hydrogen pressure.

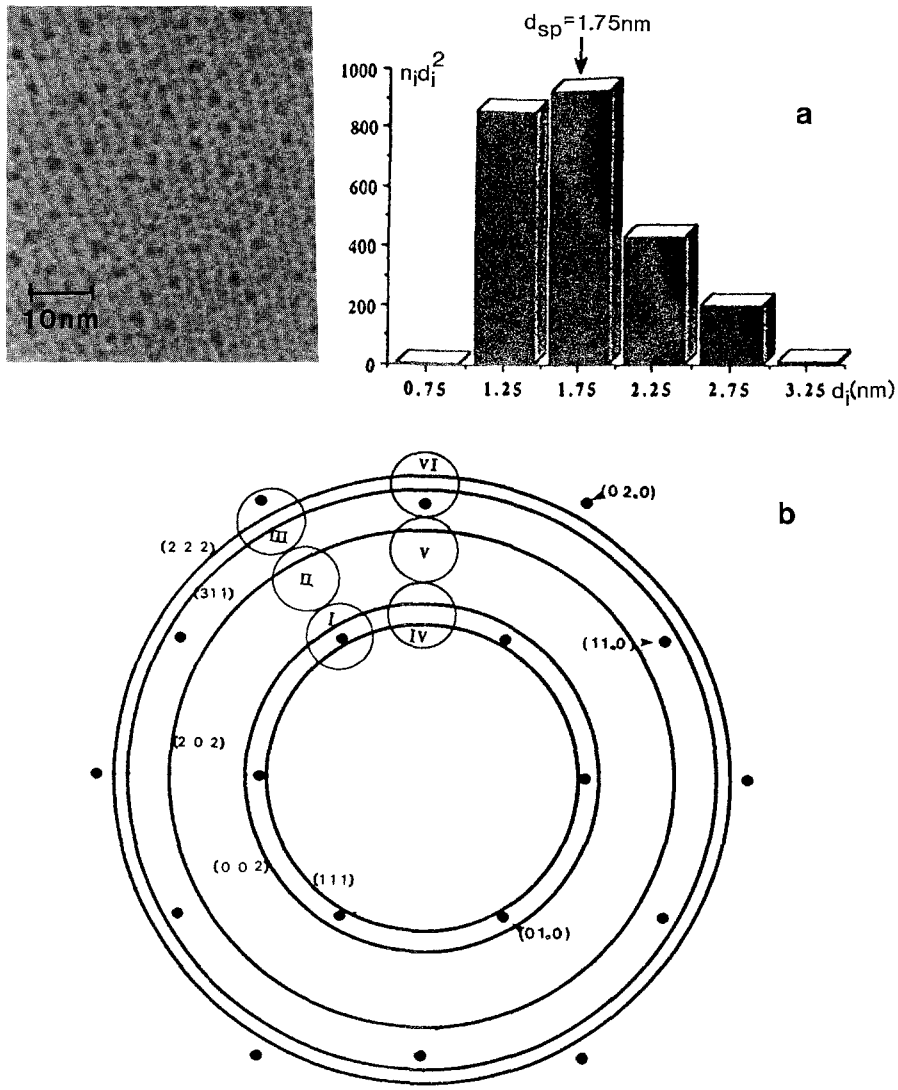

FIG. 7. (a) TEM micrograph of a Pd/graphite sample with a coverage of 8.5×10^{14} atoms $\cdot$ cm^{-2} and particle size distribution of this sample. (b) Drawing indicating the relative positions of the graphite spots for a {00.1} orientation, and of the bulk palladium spatial frequencies. In particular, the {202} plane rings ought to be separated from the {11.0} graphite spots.

(due primarily to the large spatial frequency used), one can clearly observe these particles and see that their density is comparable with the one observed on the bright field image. This means that no {111} or {002} palladium diffract and that the {202} planes do. This points to a ⟨111⟩ orientation (ternary axis) for the palladium particles. Furthermore, there is a good epitaxy between the graphite substrate and the deposited particles: $\langle 111\rangle_{Pd}//\langle 00.1\rangle_{Gr}$ and $\{202\}_{Pd}//\{11.0\}_{Gr}$. Finally the palladium parameter is different from the bulk palladium: the aperture used in position VI does not include the position of bulk palladium {202} spot, while aperture V (which did not give any Pd particles) does. This fact, added to the diffraction pattern where no palladium spot is seen near the

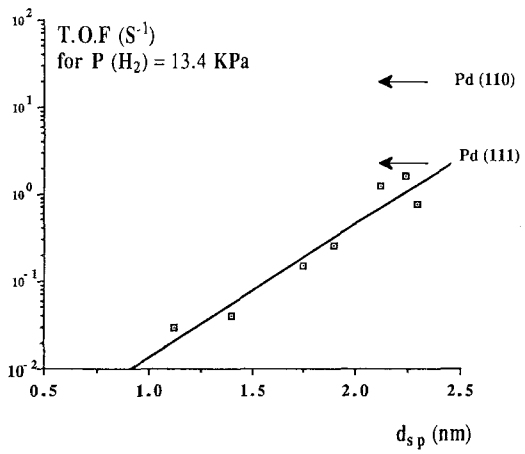

FIG. 8. 1,3-Butadiene hydrogenation reaction on Pd particles deposited on graphite. TOF variations versus mean diameter d_{sp}.

graphite {11.0}, though from the dark field image there ought to be one, could mean that the {202} palladium spots have moved toward the {11.0} graphite spots. This points to a decrease of the palladium parameter (increase in spatial frequency) with the distance between two neighbor atoms in the palladium (normally 0.27 nm in bulk) tending toward the distance of two closest atoms in graphite (0.246 nm).

Catalytic reaction. With respect to the catalytic hydrogenation of 1,3-butadiene, Pd particles deposited on graphite behave similarly to Pd aggregates on amorphous carbon. The catalytic activity increases when the particle size increases (Fig. 8). The activity per surface atom reaches a value similar to that determined on Pd single crystals (*18*). Only butenes were primarily produced, and the selectivity remained near unity up to very high conversion.

The particle size (and TOF) determinations have been based on the curve of the Fig. 3 which gives the particle size versus the Pd coverage established for deposits on amorphous carbon. The validiy of such a relation has been verified by analysis of TEM images obtained from some deposits on the graphitic support.

Vibrational EELS results. EELS observations have been done on the Pd/graphite aggregates after the 1,3-butadiene hydrogenation and evacuation. Structures characteristic of hydrocarbon residues are evidenced, corresponding to CH stretching modes near 2980 cm^{-1} and CH, CH_2, and (or) CH_3 deformation modes near 1430 and 765 cm^{-1}, for the larger Pd particles only (Fig. 9). No peaks emerge from the background in the spectra measured after reaction on the smaller particles ($d_{sp} \approx 1.4$ nm). Moverover, after CO adsorption a loss peak corresponding to the excitations of the CO stretching mode is evidenced at 1900 cm^{-1} for the larger Pd particles. Its energy is the same as that measured for CO chemisorbed on Pd single crystals (*22*). Its intensity diminishes and its energy shifts slightly toward lower values, when the Pd particle size decreases. For the smaller particles, the observation of the CO stretching mode is no longer possible. The nonobservation of molecular vibration modes cannot be explained by a lack of sensitivity associated to the diminution of the metallic area for the smaller with respect to the larger particles; indeed, in the considered particle size range, the metallic area is only changed by a factor of four. It is indicative of either no adsorption at all, or a completely dissociative adsorption on the smaller particles.

DISCUSSION

In the experimental conditions used to make the deposits (low atomic Pd flux, 300 K for the temperature of the support), the Pd particles exhibit a narrow size distribution whatever the carbonaceous support, graphite or amorphous carbon. TEM studies do not allow a precise determination of the structure and shape of the smaller aggregates. For particles in the 2-nm diameter range many possible crystallographic orientations of the bulk structure are still evidenced on the amorphous carbon support. Many of them exhibit the fcc structure. But, high resolution TEM observations indicate the presence of some metallic particles hav-

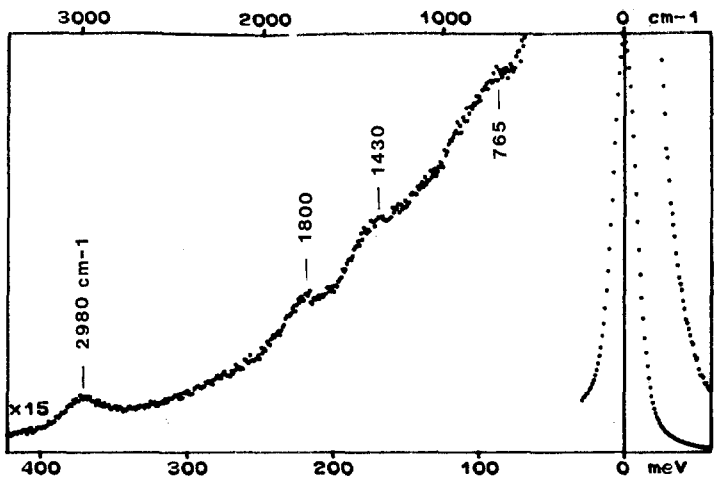

FIG. 9. EELS spectrum after 1,3-butadiene hydrogenation on Pd/graphite (particle diameter d_{sp} = 2.1 nm). Primary energy = 3 eV.

ing a C_5 symmetry axis. On the graphitic support, all the aggregates have their ⟨111⟩ ternary axis perpendicular to the basal plane of the graphite.

With respect to the catalytic behavior of Pd particles deposited on carbonaceous supports, important changes are evidenced in the d_{sp} = 2.8 to 1.4-nm size range (which corresponds to a geometric mean diameter of 2.5 to 1.2 nm). Such a result can be closely compared to data gained on Pd particles vapor deposited on another support, SiO_2 (*23*).

The very low reactivity of the smaller Pd particles for the 1,3-butadiene hydrogenation reaction in the experimental conditions used (300 K, $PH_2 \approx 50$ Torr, $PC_4H_6 \approx 5$ Torr) could be due either to an intrinsic lack of activity or to a rapid deactivation. In order to state clearly what alternative proposal must be retained, complementary measurements have been performed in experimental conditions which must lead to a less rapid deactivation, i.e., higher hydrogen pressure (100 Torr) and lower diene partial pressure (1 Torr). In such experimental conditions, the smaller Pd particles studied ($d_{sp} \approx 1.4$ nm) are active; the TOF determined then for the hydrogenation of 1,3-butadiene to butenes reaches 6 s^{-1}, a value quite comparable to that determined for the larger Pd particles and massive Pd. But, upon repeating the batch reaction run without further cleaning of the samples, the activity is found to decrease fast down to the steady state value previously reported for the TOF.

It must be noted that very small particles ($d_{sp} \approx 1.2$ nm) prepared by classical chemical ways only slightly deactivate at the very beginning of the reaction process, and exhibit a noticeable activity for the 1,3-butadiene hydrogenation reaction even at low hydrogen pressure and high contents of hydrocarbon (*17, 18, 24*). While the deactivation appears to be quite general for the hydrogenation reactions of unsaturated hydrocarbons, its amplitude would depend upon the preparation procedure of supported metal catalysts, leading to different kinds of supported metal particles: Pd aggregates obtained by atomic beam deposition techniques would behave in a special way for this purpose. A tentative explanation could be that these Pd particles vapor deposited on a support maintained at low temperature would be in a metastable state, thus having an excess of energy easily transferred to the adsorbed reactants. The thermal treatments applied during the reduction processes of more conventional metal catalysts could play a major role on the morphol-

ogy and structure of the metal particles, so obtained. The lack of observation of vibration modes characteristic of CH (and CO) groups in vibrational EELS spectra on the smaller Pd particles put in contact with unsaturated hydrocarbons (and carbon monoxide) further support that conclusion. Indeed, it seems that a complete dissociation of admolecules has followed the chemisorption. This must be compared to previous data reporting that CO chemisorbs more strongly on smaller Pd particles prepared by vapor deposition on various supports (*9*). During the 1,3-butadiene hydrogenation reaction the very small vapor deposited Pd particles would be covered by carbon and thus be rendered inactive.

Electronic effects associated with the small size of the Pd particles prepared by atomic beam deposition techniques must therefore be invoked to explain the reactivity changes experimentally observed. From XPS measurements, performed on Pd particles after the hydrogenation reaction, a shift upward of the Pd $3d_{5/2}$ binding energy and a significant increase of the linewidth are evidenced for the smaller particles (*24*). Such an observation seems general and only a little dependent upon the nature of the support: SiO_2 (*25, 26*); C (*6, 27*); Al_2O_3 (*26*). Although there is no consensus to date on whether the initial state or the final state effect is responsible for the observed shift, complementary information gained by X-ray adsorption spectroscopy (XAS) (*6*) and by Auger electron spectroscopy (AES) (*26*) tends to indicate that the size sensitivity of the XPS binding energies would be dominated by the initial state properties for weakly interacting substrates. These changes of the electronic structure with the metal particle size would be responsible for the deactivation via a too strong interaction with the 1,3-butadiene. In addition, experiments indicate that, while less important, surface structure effects can exist; this is clear from single crystal studies (*18*). For Pd particles supported on the carbonaceous supports here employed, electron diffraction and high resolution microscopy using TEM clearly indicate that the orientation of particles differs on amorphous carbon, on which the presence of many orientations have been evidenced, and on graphite, on which the ⟨111⟩ axis perpendicular to the surface of the support dominates for the particles. Moreover an additional epitaxial strain is imposed to the Pd particles on the graphite support. Both phenomena, preferential orientation and epitaxial strain effects, can be tentatively invoked to explain the lower diminution of the reactivity for the 1,3-butadiene hydrogenation reaction versus the particle size of Pd vapor deposited on graphite as compared to Pd supported on amorphous carbon. But the main phenomenon (i.e., the very large diminution of reactivity appearing between 2.8 and 1.4 nm for the Pd particle size) cannot be explained when considering only these geometrical points.

CONCLUSION

In conclusion, the reactivity of model Pd catalysts obtained by condensation of metal atoms on amorphous carbon and pyrolytic graphite for the 1,3-butadiene hydrogenation reaction is size dependent. Metal particles larger than 2.8 nm behave like bulk palladium. The size effect is marked in the 2.8 to 1.4 nm specific diameter range. The steady-state activity of lower size Pd particles can be very small due to a rapid deactivation. This effect appears to be more pronounced on Pd aggregates prepared by atomic-beam deposition techniques than on Pd catalyts prepared by more classical ways. In addition, more subtle changes do occur associated to geometric effects, and structural properties which can be induced by an epitaxial relation between the support and the active metal. Complementary studies must now be undertaken to precisely determine the morphology and structure of the small Pd aggregates prepared by vapor deposition.

ACKNOWLEDGMENT

The authors are very grateful to S. Nitsch for his help in the electron microscopy experiments.

REFERENCES

1. Poppa, H., Lee, E. H., and Moorhead, R. D., *J. Vac. Sci. Technol.* **15,** 1100 (1978).
2. Gillet, M., *Surf. Sci.* **67,** 139 (1977).
3. Chapon, C., Henry, C. R., and Chemam, A., *Surf. Sci.* **162,** 747 (1985).
4. Heineman, K., Osaka, T., Poppa, H., and Avalos-Borja, M., *J. Catal.* **83,** 61 (1983).
5. Gordon, M. B., Ph.D. thesis, Grenoble, 1978.
6. Mason, M. G., *Phys. Rev. B* **27,** 748 (1983).
7. Parks, E. K., Weiller, B. N., Bechthold, P. S. Hoffman, W. F., Nieman, G. C., Pobo, L. G., and Riley, S. J., *J. Chem. Phys.* **88,** 1623 (1988).
8. Zakin, N. R., Cox, T. M., and Kaldor, A., *J. Chem. Phys.* **89,** 1201 (1988).
9. Chou P., and Vannice, M. A., *J. Catal.* **104,** 17 (1987).
10. Masson, A., Bellamy, B., Colomer, G., M'Bedi, M., Rabette, P., and Che, M., *in* "Proceedings, 8th International Congress on Catalysis, Berlin, 1984," Vol. 4, p. 333. Dechema, Frankfurt-am-Main, 1984.
11. Masson, A., Bellamy, B., Hadj Romdhane, Y., Che, M., and Dufour, G., *Surf. Sci.* **173,** 479 (1986).
12. Hadj Romdhane, Y., Bellamy, B., Degouveia, V., Masson, A., and Che, M., *Appl. Surf. Sci.* **31,** 383 (1988).
13. Bellamy, B., Ph.D. thesis, Paris, 1987.
14. Boitiaux, J. P., Cosyns, J., and Vasudevan, S., *Appl. Catal.* **6,** 41 (1983); *in* "Preparation of Catalysts II," p. 12. Elsevier, Amsterdam, 1983.
15. Boitiaux, J. P., Cosyns, J., and Martino, G., *in* "Metal-Support and Metal-Additive Effects in Catalysis," p. 335. Elsevier, Amsterdam, 1982.
16. Sarkany, A., Weiss, A. H., and Guczi L., *J. Catal.* **98,** 550 (1986).
17. Ouchaïb, T., thesis UCB-LYON, 1989.
18. Massardier, J., Bertolini, J. C., and Renouprez, A., *in* "Proceedings, 9th International Congress on Catalysis, Calgary, 1988" (M. J. Phillips and M. Ternan, Eds.), Vol. 3, p. 1222. Chem Institute of Canada, Ottawa, 1988.
19. Bellamy, B., and Colomer, C., *J. Vac. Sci. Technol.* **A2,** 1604 (1984).
20. Van Hardevelt, R., and Hartog, F., *Surf. Sci.* **15,** 189 (1969).
21. Cosyns, J., *in* "Catalyse par les métaux" (B. Imelik, G. A. Martin, and A. Renouprez, Eds.), p. 371. Editions du CNRS, 1984.
22. Bradshaw, A. M., Hoffmann F. M., *Surf. Sci.* **72,** 513 (1978).
23. De Gouveia, V., Bellamy, B., Hadj Romdhane, Y., Masson, A., Che, M., *Z. Phys. D. Atoms Mol. Clusters* **12,** 587 (1989).
24. Bertolini, J. C., Delichère, P., Massardier, J., and Tardy, B., *Catal. Lett.* **6,** 215 (1990).
25. Takasu, Y., Unwin, R., Tesche, B., Bradshaw, A. M., and Grunze, M., *Surf. Sci.* **77,** 219 (1978).
26. Kohiki, S., *Appl. Surf. Sci.* **25,** 81 (1986).
27. Fuggle, J. C., Campagna, M., Zolnierek, Z., and Lasser, R., *Phys. Rev. Lett.* **45,** 1597 (1980).